

Control of resistive wall modes in a cylindrical tokamak with radial and poloidal magnetic field sensors

John M. Finn

30th November 2004

Theoretical Division, Los Alamos National Laboratory, Los Alamos, NM 87545

Motivation

Feedback stabilization of resistive wall modes: Several recent papers (Bondeson et al., Nucl. Fusion 2002; Chu, Chance, Glasser and Okabayashi, Nucl. Fusion 2003; Chu et al., Phys. Plasmas this June) have concluded, based on linear toroidal simulations (MARS, DCON) that poloidal magnetic field sensors work better than radial sensors, and that this is related to excitation of harmonics.

Approach

- Objective: to get more analytic understanding of the simulations
- Linear cylindrical equations
- Localization of sensor coils and feedback coils represented by excitation functions $f(\theta)$, $g(\theta)$ and their Fourier coefficients f_m , g_m
- Ideal plasma - resistive wall modes: plasma response can be represented by *plasma stability index*

$$\kappa_m \equiv -\psi'_m(r_w-) / \psi_m(r_w)$$

Basic equations

$$\psi'_m(1+) = -A_m\psi_m(1) + B_m\psi_m(w). \quad (1)$$

Plasma stability index κ_m : integrate $\gamma = 0$ eqs. to the resistive wall

$$\psi'_m(1-) = -\kappa_m\psi_m(1). \quad (2)$$

The thin resistive wall boundary condition

$$\gamma\tau\psi_m(1) = \psi'_m(1+) - \psi'_m(1-), \quad (3)$$

Combining,

$$(\gamma\tau + A_m - \kappa_m)\psi_m(1) = B_m\psi_m(w). \quad (4)$$

Feedback with idealized coils

- Review of linear results of J. M. Finn and L. Chacon, *Phys. Plasmas* **11**, 1866 (2004)
- Idealized coils – sense a single Fourier harmonic and feedback with a single harmonic
- Cylindrical geometry
- Proportional real gain based on radial sensors is effective and is equivalent to a more closely fitting conducting wall
- Imaginary gain ($\pi/2$ phase shift) is equivalent to plasma rotation
- Imaginary gain with two resistive walls is equivalent to “fake rotating wall”

Feedback with non-idealized coils

$$S_s = \frac{1}{2\pi} \int_{-\pi}^{\pi} \psi(1, \theta) f(\theta) d\theta, \quad (5)$$
$$S_s = \sum_m \psi_m(1) f_{-m}.$$

We take the linear proportional feedback circuit current: $I_c = -GS_s$

$$\psi(w, \theta) = I_c g(\theta) = -GS_s g(\theta), \quad (6)$$

$$\psi_m(w) = -Gg_m \sum_{m_1} \psi_{m_1}(1) f_{-m_1}, \quad (7)$$

$$(\gamma\tau + A_m - \kappa_m) \psi_m(1) = -GB_m g_m \sum_{m_1} \psi_{m_1}(1) f_{-m_1}. \quad (8)$$

Radial sensors

Two-sideband coupling:

$$\begin{aligned}\gamma\tau a_{-1} &= \lambda_{-1}a_{-1} - G\epsilon(\epsilon a_{-1} + a_0 + \epsilon a_1), \\ \gamma\tau a_0 &= \lambda_0 a_0 - G(\epsilon a_{-1} + a_0 + \epsilon a_1), \\ \gamma\tau a_1 &= \lambda_1 a_1 - G\epsilon(\epsilon a_{-1} + a_0 + \epsilon a_1).\end{aligned}\tag{9}$$

1-sideband special case ($\lambda_{-1} = \lambda_1$):

$$\begin{aligned}\gamma\tau a_0 &= \lambda_0 a_0 - G(a_0 + 2\epsilon a_1), \\ \gamma\tau a_1 &= \lambda_1 a_1 - G\epsilon(a_0 + 2\epsilon a_1).\end{aligned}\tag{10}$$

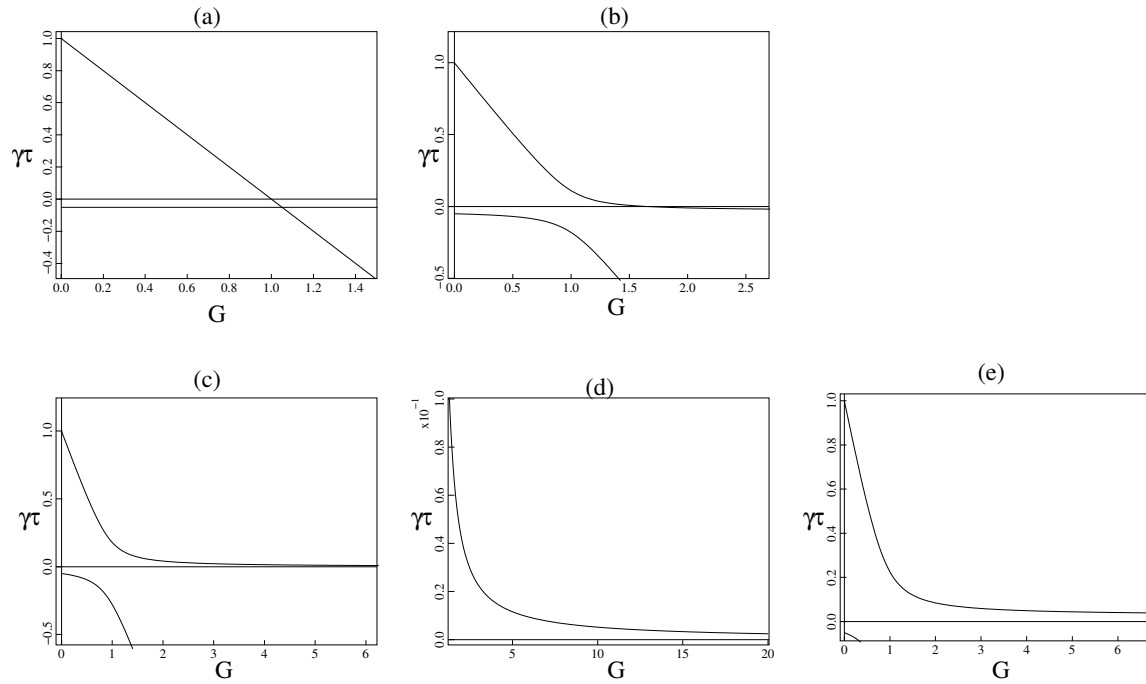


Figure 1: γ as a function of G with radial sensors; $\epsilon = 0, 0.1, \epsilon_{crit} = 0.1581$ (2) and $\epsilon = 0.2$. For $\epsilon \geq \epsilon_{crit}$ no stabilization even for $G \rightarrow \infty$. For *internal poloidal* sensors, $K = G/2$, $\epsilon = 0.0, 0.1451, 0.2294$ (2) and $\epsilon = 0.2902$.

Internal poloidal sensors

$$S_s = \sum_m \psi'_m(1-) f_{-m} \text{ and}$$

$$\psi_m(w) = K g_m \sum_{m_1} \psi'_{m_1}(1-) f_{-m_1}$$

$$(\gamma\tau + A_m - \kappa_m) \psi_m(1) = -K B_m g_m \sum_{m_1} \kappa_{m_1} \psi_{m_1}(1) f_{-m_1}.$$

Two-sideband model again:

$$\begin{aligned} \gamma\tau a_{-1} &= \lambda_{-1} a_{-1} - K \epsilon_\theta (\epsilon_\theta \kappa_{-1} a_{-1} + \kappa_0 a_0 + \epsilon_\theta \kappa_1 a_1), \\ \gamma\tau a_0 &= \lambda_0 a_0 - K (\epsilon_\theta \kappa_{-1} a_{-1} + \kappa_0 a_0 + \epsilon_\theta \kappa_1 a_1), \\ \gamma\tau a_1 &= \lambda_1 a_1 - K \epsilon_\theta (\epsilon_\theta \kappa_{-1} a_{-1} + \kappa_0 a_0 + \epsilon_\theta \kappa_1 a_1). \end{aligned}$$

Equivalent to radial sensors case with $G_{r-equiv} = K \kappa_0$ and $\epsilon_{r-equiv} = \epsilon_\theta \sqrt{\kappa_1 / \kappa_0}$.

Smaller effective coupling constant and larger effective gain.

External poloidal sensors

Two sideband model again leads to

$$\begin{aligned}\frac{\gamma\tau+1-\kappa_{-1}}{\gamma\tau-\kappa_{-1}}b_{-1} &= \widehat{K}\epsilon(\epsilon b_{-1} + b_0 + \epsilon b_1), \\ \frac{\gamma\tau+1-\kappa_0}{\gamma\tau-\kappa_0}b_0 &= \widehat{K}(\epsilon b_{-1} + b_0 + \epsilon b_1), \\ \frac{\gamma\tau+1-\kappa_1}{\gamma\tau-\kappa_1}b_1 &= \widehat{K}\epsilon(\epsilon b_{-1} + b_0 + \epsilon b_1).\end{aligned}$$

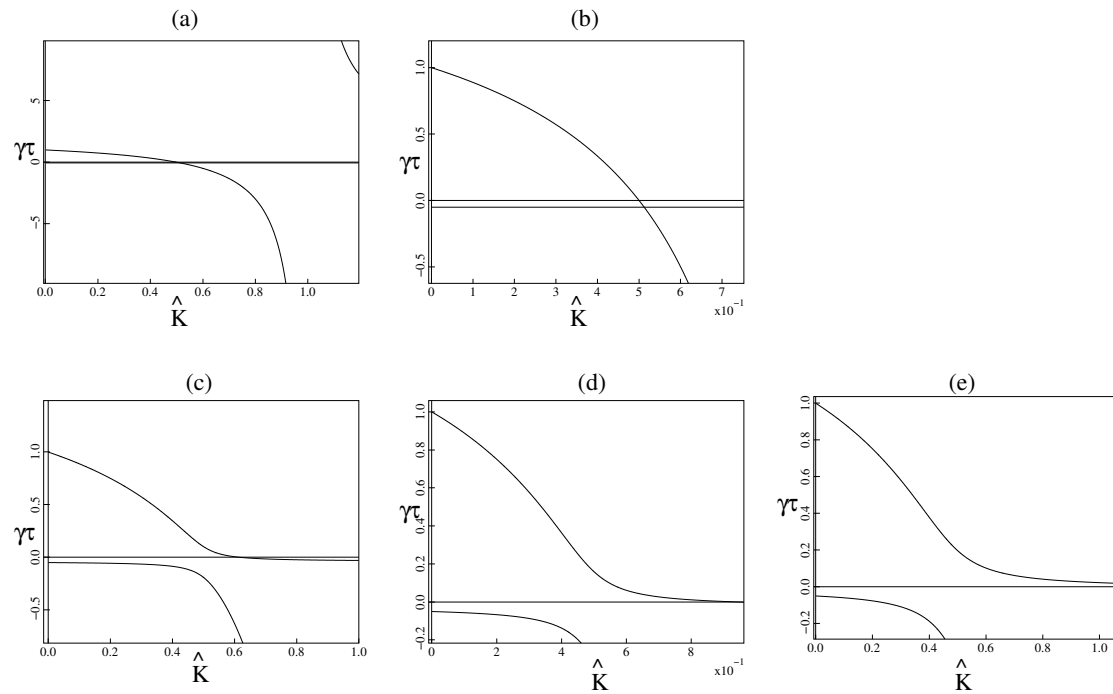


Figure 2: Growth rate as a function of the gain \hat{K} for external poloidal sensors and $\epsilon = 0$ (twice) and $\epsilon = 0.1, 0.1581, 0.2$. Results with external poloidal sensors are about as effective as those with radial sensors.

Phase shift of coils - complex gain and reduction of coupling

Sensor coil phase shift $f(\theta) \rightarrow f(\theta - \theta_0)$: $f_m \rightarrow e^{-im\theta_0} f_m$. [Phase shift of the feedback coil $g(\theta) \rightarrow g(\theta + \theta_0)$] For radial sensors,

$$(\gamma\tau + A_m - \kappa_m) \psi_m(1) = -GB_m g_m \sum_{m_1} \psi_{m_1}(1) e^{-im_1\theta_0} f_{-m_1}, \quad (11)$$

Two-sideband coupling:

$$\begin{aligned} \gamma\tau a_{-1} &= \lambda_{-1} a_{-1} - Ge^{im\theta_0} \epsilon (\epsilon e^{-i\theta_0} a_{-1} + a_0 + \epsilon e^{i\theta_0} a_1), \\ \gamma\tau a_0 &= \lambda_0 a_0 - Ge^{im\theta_0} (\epsilon e^{-i\theta_0} a_{-1} + a_0 + \epsilon e^{i\theta_0} a_1), \\ \gamma\tau a_1 &= \lambda_1 a_1 - Ge^{im\theta_0} \epsilon (\epsilon e^{-i\theta_0} a_{-1} + a_0 + \epsilon e^{i\theta_0} a_1). \end{aligned} \quad (12)$$

Two effects (if $\lambda_{-1} = \lambda_1$): $\epsilon \rightarrow \epsilon \cos \theta_0$ – less coupling.

Also $G \rightarrow Ge^{im\theta_0}$ – complex gain - equivalent to wall rotation. (However, imaginary gain without mode coupling cannot stabilize – the plasma inertia is neglected.)

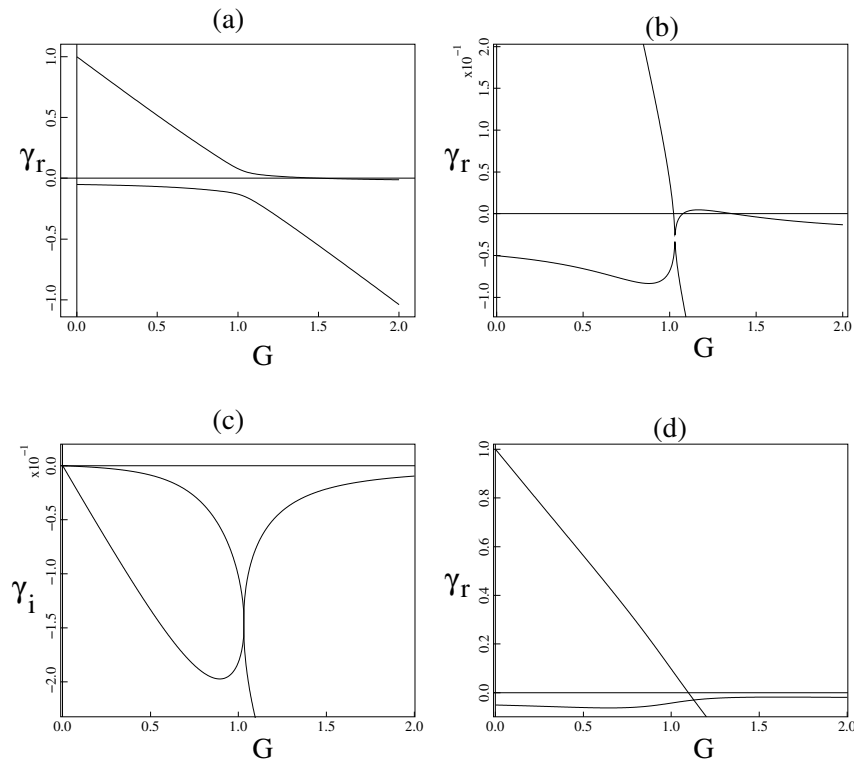


Figure 3: Growth rate γ_r and real frequency γ_i as functions of gain G for increasing $\theta_0 = \theta_1$.

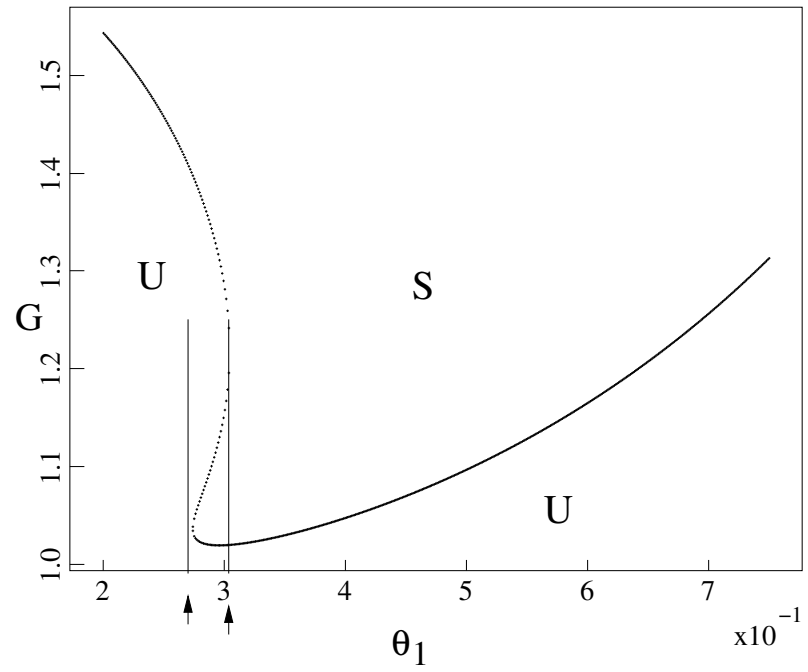


Figure 4: Stability region plot vs θ_1 and G .

Analytic model shows

- Sensor coil sensitivity to a broad spectrum of poloidal modes is equivalent to feedback coil excitation of a broad spectrum of modes.
- Broad spectrum ($\epsilon > \epsilon_{crit}$) of either sensor or feedback coil leads to the impossibility of control with radial sensors even with $G \rightarrow \infty$. Observed empirically in the simulations.
- Internal poloidal sensors are better (observed in simulations) – equivalent to radial sensors but with effective poloidal coupling smaller and effective gain larger, both good. It still is possible that coupling can prevent stabilization, but larger actual coupling ϵ_{crit} is required. External poloidal sensors are comparable in effect to radial sensors.
- Relative phase difference of sensor and feedback coils has two effects, both good: weakening of coupling and complex gain (equivalent to rotation.)